J Mater Sci: Mater Electron (2017) 28:12100–12107
DOI 10.1007/s10854-017-7023-2

Arabic gum as green agent for ZnO nanoparticles synthesis: properties, mechanism and antibacterial activity

Muneer M. Ba-Abbad[1,2,4] · Mohd S. Takriff[1,2] · Abdelbaki Benamor[3] · Ebrahim Mahmoudi[1] · Abdul Wahab Mohammad[1,2]

Received: 27 January 2017 / Accepted: 25 April 2017 / Published online: 2 May 2017

Abstract The size and morphology of ZnO nanoparticles (ZnO NPs) were controlled in the presence of the natural and green agent, Arabic gum. Lower amounts of Arabic gum showed a greater effect on the size and morphology as well as on the properties of ZnO NPs prepared by a sol–gel method. The hexagonal wurtzite crystal structure was found for all samples ZnO NPs with no other phase for impurities. The size of the spherically shaped ZnO NPs decreased with an increase in the amount of Arabic gum, up to an optimal 1.50 wt%. The smaller size of ZnO NPs of 16 nm was obtained with the optimal amount of Arabic gum, compared to 32 nm produced without Arabic gum. These results were attributed to the ready reaction between Arabic gum molecules and zinc ions within the nucleation and growth processes of ZnO NPs. The optical properties of ZnO NPs, with a band gap of 3.4 eV and enhanced intensity of blue emission, were the result of the smaller size of ZnO at the optimal amount of Arabic gum. According to the experimental results, a mechanism to elucidate the formation of ZnO NPs was proposed and explained. The antibacterial activity was tested against *Escherichia coli* against which higher activity, explained by smaller size of the ZnO NPs, was obtained.

✉ Muneer M. Ba-Abbad
muneer711@gmail.com

[1] Department of Chemical and Process Engineering, Faculty of Engineering and Built Environment, Universiti Kebangsaan Malaysia, 43600 Bangi, Selangor, Malaysia

[2] Research Centre for Sustainable Process Technology, Faculty of Engineering and Built Environment, Universiti Kebangsaan Malaysia, 43600 Bangi, Selangor, Malaysia

[3] Gas Processing Centre, Qatar University, P.O. Box 2713, Doha, Qatar

[4] Department of Chemical Engineering, Faculty of Engineering and Petroleum, Hadhramout University of Science & Technology, Mukalla, Hadhramout, Yemen

1 Introduction

Recently, zinc oxide nanoparticles (ZnO NPs) have become one of the most important commercial nanomaterials in the world. This importance is due to their multiple applications such as in photodetectors, paints, gas and biosensors, electronics, lasers, transistors, optoelectronics, solar cells, cosmetics, biomedicine, the food industry, anticorrosive coatings, antibacterial and antifungal agents and photocatalysts [1]. To apply ZnO NPs to prominent applications needs special fabrication to control the morphology and functionalisation of the surface, as well as the optical properties [2]. Two main methods of synthesis of ZnO NPs, physical and chemical, have been reported, and include evaporation, pulse laser deposition, sputtering and pyrolysis, hydrothermal, co-precipitation, and sol–gel methods [3]. All these methods could assist to control morphology (as shape, size) and properties of ZnO NPs by optimising the influence of parameters such as molar ratio, pH, calcination temperature, solvent, the presence of additives as capping agents, etc. [4]. Many previous studies have used a capping agent or a surfactant as additive to manage the size of ZnO NPs, but these additives are toxic and costly chemicals, and eradicating them from the surface of the synthesised nanoparticles would prove to be an arduous task. Therefore, large-scale production of nanoparticles would undoubtedly result in serious contamination of the environment [5]. Different additives used as capping agents, such as polyethylene glycol (PEG), polyvinyl alcohol (PVA), ethylene diamine, triethanolamine, tetraethyl ammonium bromide, glycine, gelatin and octadecyltrimethoxysilane have

been used to control the morphology and properties of ZnO NPs [6–9]. Recently, green and environmentally friendly additives as agents to assist in the control and synthesis of nanosized materials, especially ZnO NPs, have attracted much attention [10]. However, infectious bacterial diseases have become a serious human health problem worldwide and have caused many economic and social problems [11]. The modification of ZnO NPs properties, such as optical, mechanical, chemical, electrical, and structural are controlled by reductions of size and changes of morphology. These modified properties allow ZnO NPs have more reactive species on their surface and lead to significant applications in science and bionanotechnology [11]. Many researchers have reported that nanosized ZnO has significant antimicrobial activities which are attributed to the possibility of interaction with bacterial surfaces to enter into the cell [12]. Consequently, ZnO NPs have been reported as materials non-toxic to human cells, and which are considered as bio-safe materials for use in photo-oxidisation and photocatalysis processes [13]. In this work, the control of size of ZnO NPs in synthesis is by a sol–gel method in presence of Arabic gum. The Arabic gum agent is cheap, non-toxic and available on an industrial scale. This method using Arabic gum, with water as solvent, shows an environmentally friendly approach because of the use of two natural compounds as precursors. In addition, the method of preparation (sol–gel) is a simple and efficient method in the laboratory because it does not require special or complicated equipment.

2 Experimental

2.1 Materials and chemicals

Zinc nitrate hexahydrate ($Zn(NO_3)_2{\cdot}6H_2O$) supplied by BDH Prolabo chemicals was the main source of ZnO for NPs. Oxalic acid dihydrate ($C_2H_2O_4{\cdot}2H_2O$) was obtained from R&M Chemicals, Malaysia. The Arabic gum agent was ordered from Sigma-Aldrich, Malaysia. Deionised water was used as solvent for the preparation of ZnO NPs.

2.2 Synthesis of ZnO nanoparticles

The simple route of a sol–gel method was applied to synthesize ZnO NPs, with different amounts of Arabic gum as capping agent. The zinc nitrate and oxalic acid dihydrate were used as starting materials dissolved in water. Separate solutions of zinc nitrate and oxalic acid in molar ratio 1:2 were prepared in 100 and 50 mL water, respectively, in beakers, and stirred for 30 min at room temperature. The Arabic gum with several percentages (wt%) of 0.5, 1.5 and 3.0 was added to each solution of zinc nitrate under continuous stirring. The oxalic acid solution was added dropwise to the zinc nitrate solution under continued stirring and the stirring continued for 4 h. The mixture was dried at 80 °C overnight and the final powder was thermally treated at calcination temperatures of 400 °C for 2 h.

3 Characterizations of ZnO nanoparticles

To investigate the properties of ZnO NPs synthesized using Arabic gum, several characterizations were applied such as X-ray diffraction (Bruker D8 Advance AXS X-ray diffractometer) with Cu K-α radiation (1.5406 Å) in the 2θ scan range of 20°–80° to determine the crystal phase composition and the crystal size. To show the morphology of ZnO NPs, transmission electron microscopy (Philips CM200, model JEOLJEM 2100) was used. The optical properties of ZnO NPs, such as band gap and photoluminescence (PL) were investigated at room temperature using a Perkin Elmer (LAMBDA 35) UV/Vis spectrophotometer and a PerkinElmer LS-55125 luminescence spectrometer with a Xe lamp as the excitation 325 source.

4 Antibacterial testing

The activity against bacteria growth of ZnO NPs synthesized with and without using Arabic gum was evaluated. The antimicrobial test was achieved using Kirby–Bauer antibiotic testing, also called disc diffusion antibiotic sensitivity testing. *Escherichia coli K12* (*E. coli*) grown overnight on nutrient agar at 35 °C was used to test ZnO NPs samples for antimicrobial activity. One colony of the bacteria was transferred to the nutrient broth and incubated for 8 h to reach 1.6×10^7 cells/mL and then 20 µL of solution was spread onto nutrient agar [14, 15]. At the same time, ZnO NPs samples were prepared at 1 mg/mL in water and then 20 µL of mixture solution added to equal-sized autoclave-sterilized filter paper disks (5 mm) and left at room temperature to dry overnight. Finally, the paper disks containing the ZnO NPs samples were placed on the surface of the agar and incubated at 35 °C for 1–2 days. The inhibition zone of *E. coli* growth was measured around the paper disks (mm) [16].

5 Results and discussion

5.1 X-ray diffraction (XRD)

To investigate the phase structure and crystal size of ZnO NPs after addition of Arabic gum as capping agent, X-ray diffraction (XRD) was studied. The XRD patterns

of ZnO NPs before and after addition of Arabic gum are shown in Fig. 1. All samples of ZnO NPs show that a wurtzite structure with hexagonal phase was produced, which in good agreement with the standard card JCPDS 36-1451 which 2θ at 31.68°, 34.36°, 36.18° and 56.56° corresponding to the (100), (002), (101) and (110) plane, respectively. The ZnO NPs without Arabic gum exhibited a larger crystal size (29 nm), according to the higher intensity and sharpness of all peaks, as presented in Fig. 1a. The crystal size of ZnO NPs decreased from 24 to 14 nm when Arabic gum addition increased from 0.5 to 1.5 wt%, with a slight increase to 19 nm with addition of 3.0 wt%. The decrease in size of ZnO NPs was confirmed by the inhibition of peak intensity and that peaks became broader, as shown in Fig. 1b. The smallest crystal size, at optimal additive amount of Arabic gum of 1.5 wt%, may be attributed to the faster particle growth, as reported in earlier work [17]. However, when the amount increased to 3.0 wt%, the particle size increase may be due to the additional amount of Arabic gum producing a stable Zn^{2+} complex with the gum, causing a slowing of growth of the ZnO NPs [18].

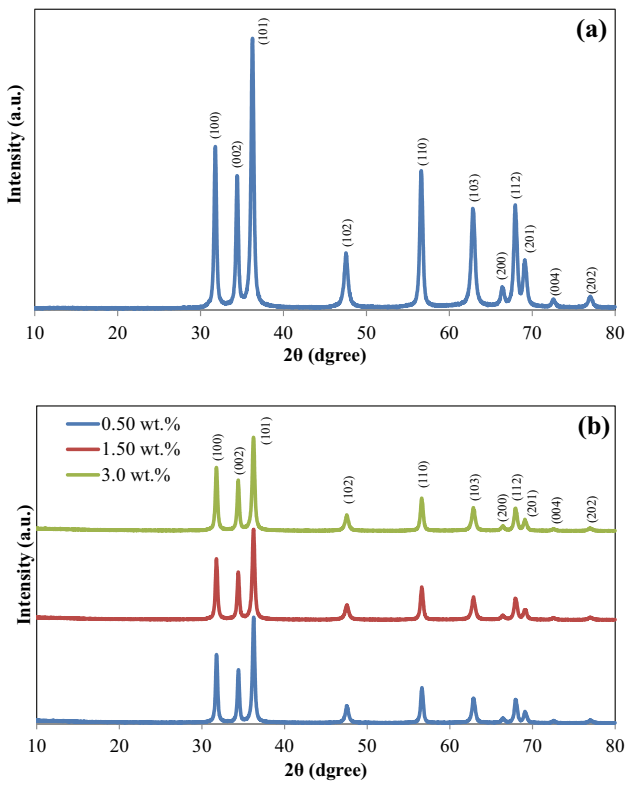

Fig. 1 XRD of ZnO NPs synthesized with Arabic gum **a** 0.00 wt% and **b** with several wt% of Arabic gum

5.2 Transmission electron microscopy (TEM)

The effect of different wt% of Arabic gum on ZnO NPs morphology, shape and particle size was investigated using TEM. Figure 2 shows the morphology of ZnO NPs before and after addition of Arabic gum and its effect on particle size. The almost spherical shapes of different sizes of both samples before and after Arabic gum addition were observed. The sizes of ZnO NPs decreased when amount added increased from 0.5 to 1.5 wt% and then increased at 3.0 wt%. The average particle sizes of 32, 25, 16 and 21 nm were found for 0.0, 0.5, 1.5 and 3.0 wt% of Arabic gum respectively, which is consistent with the results from XRD analysis. The TEM results showed that the adsorption of Arabic gum molecules on the surface of NPs plays a main role in, or is the main reason for, the stabilization and growth control of NPs [19]. The optimum amount Arabic gum addition was found to be 1.5 wt%, at which the lowest size of 16 nm was produced. When the Arabic gum was higher than optimum, the particle size was increased, which is attributed to agglomeration of smaller particles, producing slightly larger particles under heat treatment [20]. Further discussion of the mechanism of growth of NPs using Arabic gum will appear in the next section.

5.3 Optical properties (band gap and photoluminescence)

The effect of different amounts of Arabic gum on the optical properties, such as band gap and photoluminescence, of ZnO NPs is shown in Fig. 3. The band gap of all ZnO NPs samples was calculated from Fig. 3a by the equation:

$$\alpha h\nu = A\,(h\nu - E_g)\;1/2 \tag{1}$$

where hν is the photon energy, α is the optical absorption coefficient, E_g is the direct optical band gap, and A is a material-dependent constant [21]. The band gap of ZnO NPs was strongly affected by the particle sizes that were produced using different wt% of Arabic gum. The band gaps were found to be 3.20, 3.40 and 3.25 eV for 0.50, 1.50 and 3.0 wt% of Arabic gum, respectively, compared to 3.16 eV for no Arabic gum. These band gap values show the influence of particle size, which affects the ability of the ZnO NPs to absorb UV light [22]. For most applications of ZnO NPs, the suitable band gap can be estimated to be between 3.0 and 3.4 eV at room temperature [23]. The photoluminescence (PL) spectra of all ZnO NPs samples at room temperature were taken and are given in Fig. 3b. Three main peaks of samples, with and without Arabic gum, were observed. These peaks may due to the band-to-band excitation of ZnO promoting electron transfer from the valence band to the conduction band. However, the first

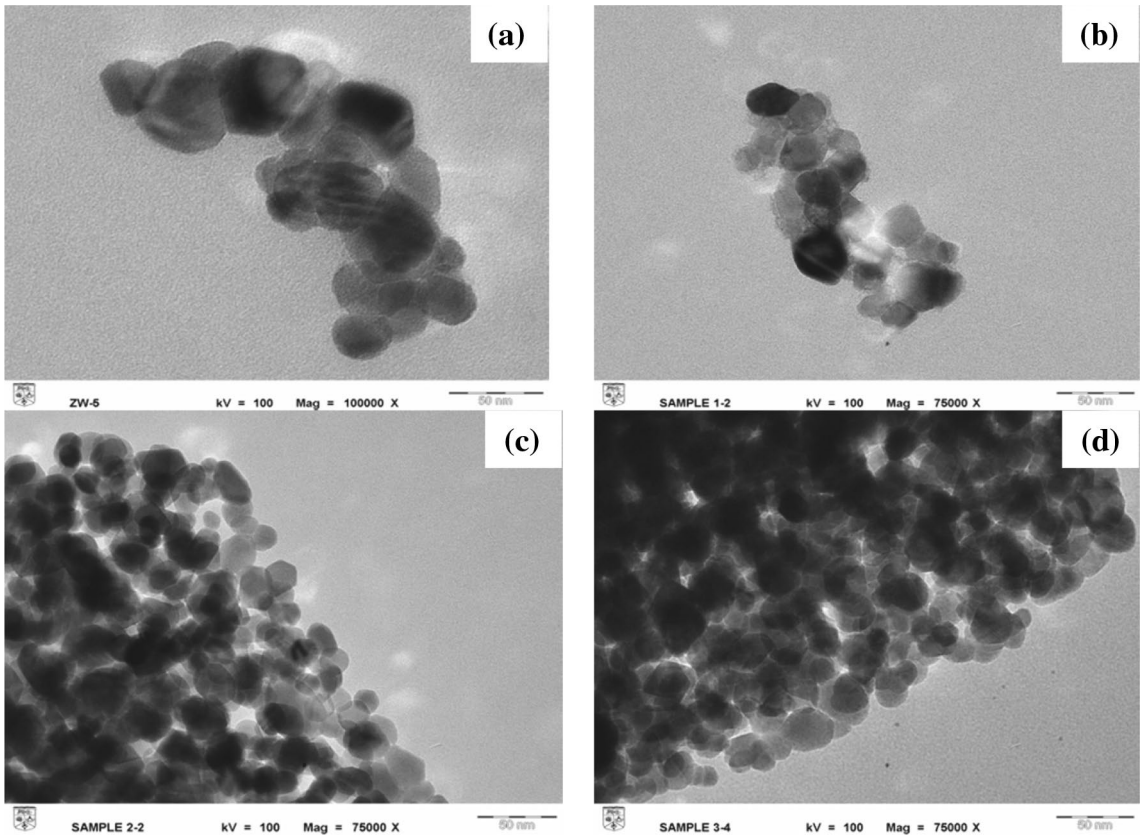

Fig. 2 TEM of ZnO NPs synthesized with Arabic gum **a** 0.00 wt%, **b** 0.50 wt%, **c** 1.50 wt%, **d** 3.0 wt%

peak at 398 nm exhibits that characteristic emission of ZnO which can be attributed to the band edge emission or excitation transition [24]. The second peak at 410 nm is associated to the electron transition from a shallow donor level of interstitial zinc (Zni) to the top level of the valence band [25]. The third peak, around 440 nm, was blue emission, which is attributed to the defect emission of interstitial zinc (Zni) [26]. Overall, from the PL spectra it can be observed that the intensity increased with Arabic gum up to 1.50 wt% then decreased. The enhancement of the intensity may due to the increase in oxygen vacancies by addition of Arabic gum compared to samples without [27]. On the other hand, the slight blue shift in UV emission can be attributed to the reduction of tensile strain when the size of ZnO NPs was decreased [27]. Additionally, the PL showed the dependence of the optical properties of ZnO NPs on size. The key role in visible emission is faster trapping, to generate holes at the surface site, followed by these tunnelling back into oxygen vacancies in the bulk ZnO. The decrease in the tunnelling rate of surface-trapped holes to oxygen vacancy centres with increasing particle size has been reported earlier [28]. This phenomenon leads to the visible emission intensity decreasing when the particle size increased, as was the case of additions of 0.00 and 3.0 wt% Arabic gum which resulted in particle sizes of 32 and 25 nm, respectively. The optical properties of ZnO NPs prepared using Arabic gum can be controlled by their morphology, these properties indicating their application.

5.4 Mechanism of control of ZnO NPs using Arabic gum

The reaction conditions in the synthesis of ZnO NPs by including different wt% of Arabic gum affect the size and stabilty of the NPs. Based on the XRD, TEM and UV–Vis, using Arabic gum to control the size of ZnO NPs plays a potential role in the synthesis process. The effect of capping agents on the mechanism of ZnO formation depending on the reacting agent has been reported [29]. In a previous study, a strong alkaline agent such as NaOH used in the presence of Arabic gum produced ZnO of non-uniform shape and size [30]. In this work, the acid used was oxalic acid, which produced uniform spherically shaped ZnO NPs with a reduction in size from 32 to 16 nm by addition of very low amount of Arabic gum (1.50 wt%). The faster release of $C_2O_4^{2-}$ ions in aqueous solution leads to both the nucleation and growth steps of ZnO being faster, which produced ZnO of smaller size compared to the process

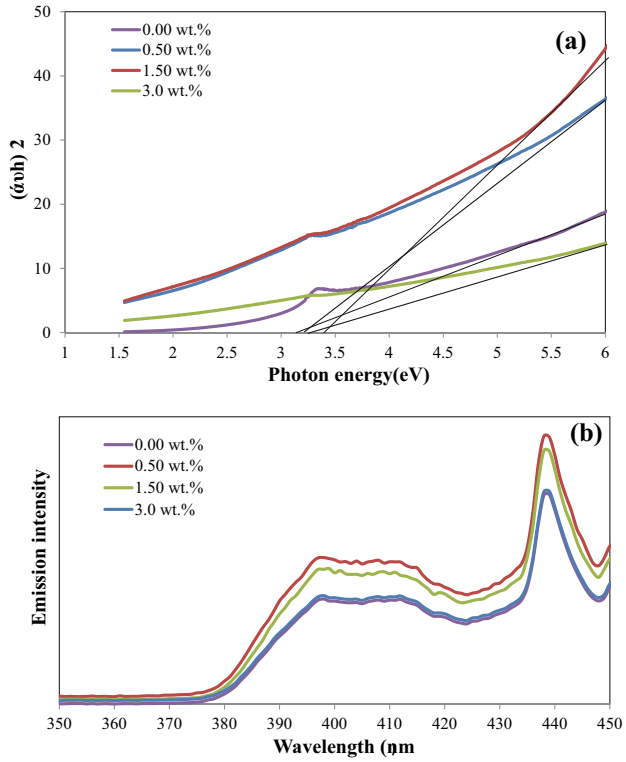

Fig. 3 Optical properties of synthesized ZnO NPs using Arabic gum, **a** band gap and **b** photoluminescence (PL)

without Arabic gum [31] (TEM results, Fig. 2). The large chains of Arabic gum are natural polysaccharides, which form complexes with Zn^{2+} ions which interact with functional groups such as –COOH, –OH and $–NH_2$ [32]. The complexes formed lead to the prevention of excess growth, producing ZnO NPs of smaller size. The simple explanation of the mechanism of formation and growth of ZnO in the presence of Arabic gum can be the following:

$$Zn\left(NO_3\right)_2 \xrightarrow{Aqueous\ solution} Zn^{2+} + 2NO_3{}^- \quad (2)$$

$$Zn^{2+} + AG \xrightarrow{Aqueous\ solution} [Zn(AG)]^{2+} \quad (3)$$

$$[Zn(AG)]^{2+} + 2\left[C_2O_4\right]^{2-} \xrightarrow{Aqueous\ solution} \left[ZnC_2O_4(AG)\right] \quad (4)$$

$$\left[ZnC_2O_4(AG)\right] \xrightarrow{Heat\ Treatment} ZnO + CO + CO_2 \quad (5)$$

The synthesis of ZnO NPs in the presence of Arabic gum showed that aggregation of ZnO NPs increases when the amount of Arabic gum was increased (TEM results, Fig. 2c, d). The lower aggregation of particles with a lower amount of Arabic gum (0.50 wt%) was observed, which was due to a small layer of Arabic gum covering the particles, allowing fewer particles to stick together within the growth step, according Eqs. 3, 4 and Fig. 2b [33]. At a higher amount of Arabic gum, a higher aggregation of particles was observed, which may be due to an increase in the layer on the surface of particles, leading to crossing the point of flocculation of many particles, as shown in TEM image (Fig. 2c, d). The adsorption of Arabic gum on the surface of ZnO NPs plays a main role in the control of growth of ZnO NPs, as reported previously [20]. The proposed mechanism of growth of ZnO NPs in the presence of Arabic gum according to the reaction and analysis of XRD and TEM is given in Fig. 4.

5.5 Antibacterial activity

The antibacterial test of ZnO NPs synthesised with and without Arabic gum was evaluated by disc diffusion antibiotic sensitivity testing using *E. coli* bacteria. Figure 5 shows the results of the inhibition zone of ZnO NPs with different amounts of Arabic gum. In general, the inhibition zone of ZnO NPs modified by Arabic gum indicated higher antibacterial activity than those ZnO NPs without Arabic gum (0.00 wt%). These results can attributed to the decreased crystal size of ZnO NPs modified by Arabic gum, as shown by XRD and TEM analysis. The highest antibacterial activity was observed in ZnO NPs prepared with 1.50 wt% Arabic gum, due to their smaller size (16 nm) and increased active surface area. Accordingly, the inhibition zone increased significantly with decreased size of ZnO NPs.

Highly reactive species of superoxide, hydrogen peroxide and hydroxyl ($O_2{}^{\bullet-}$, H_2O_2 and OH^-) were formed on the surface of ZnO activated by both UV and visible light. Electron–hole pairs ($e^- + h^+$) are created on the ZnO surface, and the hole (h^+) splits H_2O to into H^+ and $HO^\bullet$, while the dissolved oxygen is transferred to superoxide ($O_2{}^{\bullet-}$). Hence, the $O_2{}^{\bullet-}$ reacts with H^+ to generate the $HO_2{}^\bullet$ radical, which, following collision with e^-, generates $HO_2{}^-$ as the main step in the formation of H_2O_2. However, the $O_2{}^{\bullet-}$ and OH^- are negatively charged and so cannot penetrate the cell membrane and can have no influence on bacteria death. Therefore, H_2O_2 easily penetrating the bacterial cell membrane is the main reason for bactericidal action and formation of the inhibition zone [34, 35]. The steps to generate H_2O_2 are summarized below:

$$ZnO + h\upsilon\,(\lambda < 388\text{nm}) \rightarrow e^- + h^+ \quad (6)$$

$$H_2O + h^+ \rightarrow H^+ + HO^\bullet \quad (7)$$

$$O_2 + e^- \rightarrow O_2{}^{\bullet-} \quad (8)$$

$$O_2{}^{\bullet-} + H^+ \rightarrow HO_2{}^\bullet \quad (9)$$

$$HO_2{}^\bullet + e^- \rightarrow HO_2{}^- \quad (10)$$

$$HO_2{}^- + H^+ \rightarrow H_2O_2 \quad (11)$$

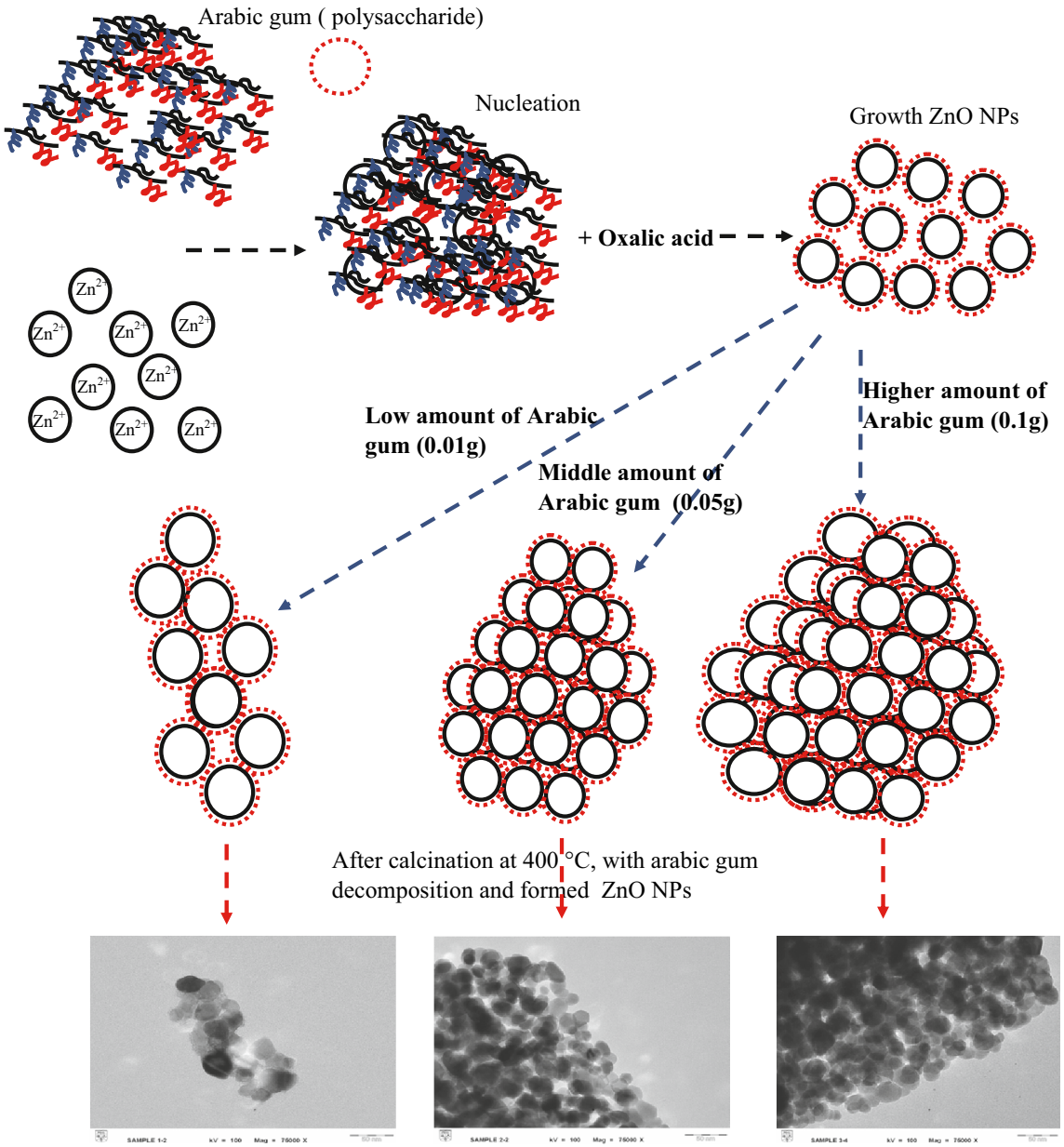

Fig. 4 Schematic diagram illustration of the effect Arabic gum amount to control ZnO NPs size

Other researchers have proposed the generation of H_2O_2 on the surface of ZnO as the main effect in the inhibition of *E. coli* bacterial growth [36, 37]. However, the smaller size of particles leads to a higher number of ZnO NPs per unit volume, resulting in increased rate of generation of H_2O_2 [38].

6 Conclusion

In summary, particle size of ZnO NPs was successfully controlled by addition of the green and natural agent Arabic gum via a sol–gel method. The XRD and TEM results showed the sizes of these ZnO NPs to be smaller than those prepared without Arabic gum. The optimal amount of Arabic gum to produce ZnO NPs of 16 nm was 1.50 wt%. The optical properties of ZnO NPs prepared with the optimal amount of Arabic gum were enhanced, and the band gap increased to 3.4 eV with the highest intensity of blue emission due to the increase in oxygen vacancies. The PL results showed the size-dependence of the optical properties of ZnO NPs. A mechanism was proposed to explain how the higher amount of Arabic gum affected an increase of agglomeration and hence the size of ZnO NPs. Using

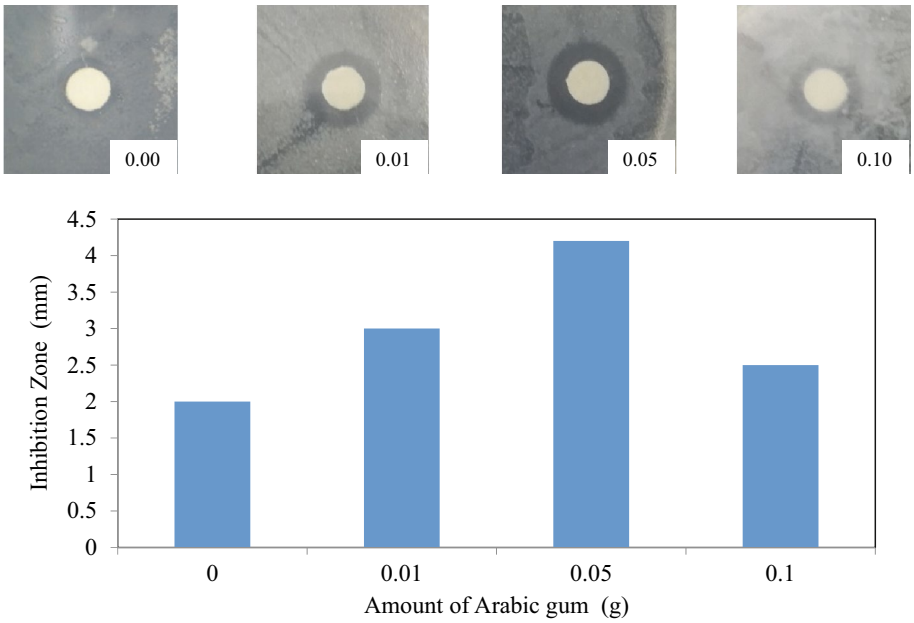

Fig. 5 Antibacterial test using disc diffusion of *E. coli* bacteria for ZnO NPs prepared with various amount of Arabic gum

this method of addition of Arabic gum, the size of ZnO NPs can be easily controlled, permitting their many applications in the future. The antimicrobial results showed that the inhibition zone increased with a decrease in the particle size of ZnO NPs. The greatest inhibition zone was observed by sizes as small as 16 nm, which can be attributed to the higher surface area, leading to the more effective generation of H_2O_2, which affects *E. coli* bacterial growth.

Acknowledgements This paper was made possible by NPRP Grant # [5-1425-2-607] from the Qatar National Research Fund (a member of Qatar Foundation) and Research Centre for Sustainable Process Technology (CESPRO), Faculty of Engineering and Built Environment, Universiti Kebangsaan Malaysia under project PKT-6/2012, iconic-2014-004. The statements made herein are solely the responsibility of the authors. One of the authors (Muneer M. Ba-Abbad) is grateful to Hadhramout University of Science &Technology, Yemen for its financial support for his PhD study. The authors would like to thank the Centre for Research and Instrumentation Management, UKM (CRIM) for XRD, TEM and PL analyses.

References

1. R.S. Shaikh, R.R. Rakh, L.S. Ravangave, Int. Res. J. Sci. Eng. **4**, 31 (2016)
2. M.M. Ba-Abbad, A.A.H. Kadhum, A.B. Mohamad, M.S. Takriff, K. Sopian, J. Alloys Compd. **550**, 63 (2013)
3. E. Maryanti, D. Damayanti, I. Gustian, S. Yudha, Mater. Lett. **118**, 96 (2014)
4. M.M. Ba-Abbad, P.V. Chai, M.S. Takriff, A. Benamor, A.W. Mohammad, Mater. Des. **86**, 948 (2015)
5. M.M. Ba-Abbad, M.S. Takriff, A.W. Mohammad, Res. Chem. Intermed. **42**, 5219 (2016)
6. A.K. Zak, W.A. Majid, M. Darroudi, R. Yousefi, Mater. Lett. **65**, 70 (2011)
7. K.S. Babu, R. Reddy, C. Sujatha, K.V. Reddy, Mater. Lett. **99**, 97 (2013)
8. J. Lee, S. Park, H. Park, J. Lee, H. Kim, Y. Chung, J. Electroceram. **22**, 100 (2009)
9. A.M. Pourrahimi, D. Liu, V. Strom, M.S. Hedenqvist, R.T. Olssona, W.U. Gedde, J. Mater. Chem. A **3**, 17190 (2015)
10. F. Davar, A. Majedi, A. Mirzaei, J. Am. Ceram. Soc. **98**, 1739 (2015)
11. A. Sirelkhatim, S. Mahmud, A. Seeni, N.H. Kaus, L.C. Ann, S.K. Bakhori, H. Hasan, D. Mohamad, Nano-Micro Lett. **7**, 219 (2015)
12. J.T. Seil, T.J. Webster, Int. J. Nanomed. **7**, 2767 (2012)
13. J.W. Rasmussen, E. Martinez, P. Louka, D.G. Wingett, Exp. Opin. Drug Deliv. **7**, 1063 (2010)
14. Q. Bao, D. Zhang, P. Qi, J. Colloid Interface Sci. **360**, 463 (2011)
15. M.M. Ba-Abbad, A.A.H. Kadhum, A.A. Al-Amiery, A.B. Mohamad, S.M. Takriff, Int. J. Phys. Sci. **7**, 48 (2012)
16. A. Mollahosseini, A. Rahimpour, M. Jahamshahi, M. Peyravi, M. Khavarpour, Desalination **306**, 41 (2012)
17. C.B. Ong, A.W. Mohammad, R. Rohania, M.M. Ba-Abbad, N.H. Hairom, Process Saf. Environ. Prot. **104**, 549 (2016)
18. Y.L. Zhang, Y. Yang, J.H. Zhao, R.Q. Tan, J. Sol–Gel Sci. Technol. **51**, 198 (2009)
19. M. B. Moreno-Trejo, M. Sánchez-Domínguez, Materials **9**, 817 (2016)
20. Y.L. López-Franco, R.E. Córdova-Moreno, F.M. Goycoolea, M.A. Valdez, J. Juárez-Onofre, J. Lizardi-Mendoza, Food Hydrocoll. **26**, 159 (2012)
21. M.M. Ba-Abbad, A.A.H. Kadhum, A.B. Mohamad, M.S. Takriff, K. Sopian, Chemosphere **91**, 1604 (2013)
22. C.H. Hung, W.T. Whang, Mater. Chem. Phys. **82**, 705 (2003)
23. Y.T. Chung, M.M. Ba-Abbad, A.W. Mohammad, A. Benamor, Desalin. Water Treat. **57**, 7801 (2016)
24. T.P. Rao, M.C.S. Kumar, N.S. Hussain, J. Alloys Compd. **541**, 495 (2012)
25. H.B. Zeng, G.T. Duan, Y. Li, S.K. Yang, X.X. Xu, W.P. Cai, Adv. Funct. Mater. **20**, 561 (2010)
26. H. Wang, S. Dong, X. Zhou, X. Hu, Y. Chang, Physica E **44**, 307 (2011)

27. Y. Wang, X. Zhao, L. Duan, F. Wang, H. Niu, W. Guo, A. Ali, Mater. Sci. Semicond. Process. **29**, 372 (2015)
28. A. van Dijken, E.A. Meulenkamp, D. Vanmaekelbergh, A. Meijerink, J. Lumin. **87**, 454 (2000)
29. M. Makkar, H.S. Bhatti, K. Singh, J. Mater. Sci. **25**, 4822 (2014)
30. M. Sulochana, C.S. Vani, D.K. Devi, N.S. Naidu, B. Sreedhar, Am. J. Mater. Sci. **3**, 169 (2013)
31. M.M. Ba-Abbad, M.S. Takriff, A. Benamor, A.W. Mohammad, Adv. Powder Technol. **27**, 2439 (2016)
32. M. Thirumavalavan, K.L. Huang, J.F. Lee, Colloids Surf. A **417**, 154 (2013)
33. K.A. Juby, C. Dwivedi, M. Kumar, S. Kota, H.S. Misra, P.N. Bajaj, Carbohydr. Polym. **89**, 906 (2012)
34. N. Padmavathy, R. Vijayaraghavan, Sci. Technol. Adv. Mater. **9**, 035004 (2008)
35. M.D. Blake, P. Maness, Z. Huang, E.J. Wolfrum, J. Huang, W.A. Jacoby, Sep. Purif. Methods **28**, 1 (1999)
36. J. Sawai, J. Microbial. Method **54**, 177 (2003)
37. M.M. Ba-Abbad, M.S. Takriff, A.A.H. Kadhum, A.B. Mohamad, A. Benamor, A.W. Mohammad, Environ. Sci. Pollut. Res. **24**, 2804 (2017)
38. O. Yamamoto, J. Inorg. Mater. **3**, 643 (2001)